

PAPER

Iterative Detection of Interleaver-Based Space-Time Codes

K. Y. WU^{†a)}, W. K. LEUNG^{†b)}, Lihai LIU^{†c)}, and Li PING^{†d)}, *Nonmembers*

SUMMARY This paper investigates a random-interleaver-based approach to space-time coding. The basic principle is to employ a good forward error correction (FEC) code and transmit randomly interleaved codewords over an antenna array. A low-cost estimation technique is considered. The complexity involved grows only linearly with the number of transmit antennas. Near-capacity performance can be achieved with moderate complexity. **key words:** *Fading channels, iterative decoding, multiple transmit antennas, space-time codes, transmit diversity.*

1. Introduction

Recently, much research effort has been devoted to space-time codes [1]-[20]. Although significant progress has been made, many challenging issues related to performance and complexity of space-time coding remain open. Some of these are listed below.

- Receiver complexity remains a serious concern. This problem arises from cross antenna interference (CAI) since signals from N transmit antennas are combined when they arrive at the receiver. The size of the arrival symbol constellation (ignoring additive noise) is Q^N , where Q is the constellation size of transmitted symbols. Even for modest Q (say, $Q = 4$ for QPSK), Q^N can be excessively large for, say, $N \geq 4$. Effective methods for addressing this issue do exist. For example, with orthogonal space-time block codes [15][16], translation techniques can be employed to reduce the size of the decision symbol constellation from Q^N to Q . However, such codes, except for the 2×2 one [15], incur a rate loss [16]. An interesting research area is therefore to search for efficient solutions when $N > 2$.
- Existing space-time coding schemes are mostly designed for specific numbers of transmit antennas. A unified design strategy for systems with an arbitrary number of transmit antennas is lacking. This is inconvenient for field deployment where the

number of transmit antennas used may vary according to the environment.

In this paper, we investigate a random-interleaver-based approach to space-time coding. The basic principle is to employ a good forward error correction (FEC) code and transmit randomly interleaved codewords over an antenna array. A repetition operation over N transmit antennas is adopted to provide diversity gain for each coded bit. Similar schemes have been studied before. In particular, the turbo-BLAST scheme in [17] is concerned with interleaved convolutional codes. The space-time turbo code in [18] also involves a random interleaver that forms part of the turbo code used. The complexities of the detection methods in both [17] and [18] grow rapidly with the number of transmit antennas N , which causes difficulties for systems with large N values.

This paper considers a turbo-type iterative receiver structure consisting of two basic processors: an elementary signal estimator (ESE) and an *a posteriori* probability (APP) decoder (DEC). The ESE provides coarse bit-by-bit estimates of the transmitted signals, which are then refined by a turbo-type iterative process involving both the ESE and the DEC. We derive a low-cost sub-optimal implementation of the ESE and show that the performance loss is marginal. As the receiver complexity increases only linearly with N , the method can be applied to systems with large numbers of transmit antennas. Near-capacity performance (only about 0.7~2dB away from the theoretical limits) is achieved.

2. System Model

Consider a transmit diversity system with N transmit antennas and one receive antenna, referred to as an $N \times 1$ system, in a quasi-static channel. We adopt a discrete-time model and denote $\boldsymbol{\alpha} \equiv [\alpha^{(1)}, \dots, \alpha^{(n)}, \dots, \alpha^{(N)}]$, where $\alpha^{(n)}$ is the fading coefficient between the n th transmit antenna and the receive antenna. Let J denote the frame length and

$$\mathbf{X} \equiv \begin{bmatrix} \mathbf{x}^{(1)} \\ \vdots \\ \mathbf{x}^{(n)} \\ \vdots \\ \mathbf{x}^{(N)} \end{bmatrix} = \begin{bmatrix} x_1^{(1)} & \cdots & x_j^{(1)} & \cdots & x_J^{(1)} \\ \vdots & & \vdots & & \vdots \\ x_1^{(n)} & \cdots & x_j^{(n)} & \cdots & x_J^{(n)} \\ \vdots & & \vdots & & \vdots \\ x_1^{(N)} & \cdots & x_j^{(N)} & \cdots & x_J^{(N)} \end{bmatrix} \quad (1)$$

Manuscript received January 13, 2004.

Manuscript revised May 17, 2004.

Final manuscript received August 1, 2004.

[†]The authors are with the Department of Electronic Engineering, City University of Hong Kong, Hong Kong

a) E-mail: kewu@ee.cityu.edu.hk

b) E-mail: wkleung@ee.cityu.edu.hk

c) E-mail: lhliu@ee.cityu.edu.hk

d) E-mail: eeliping@cityu.edu.hk

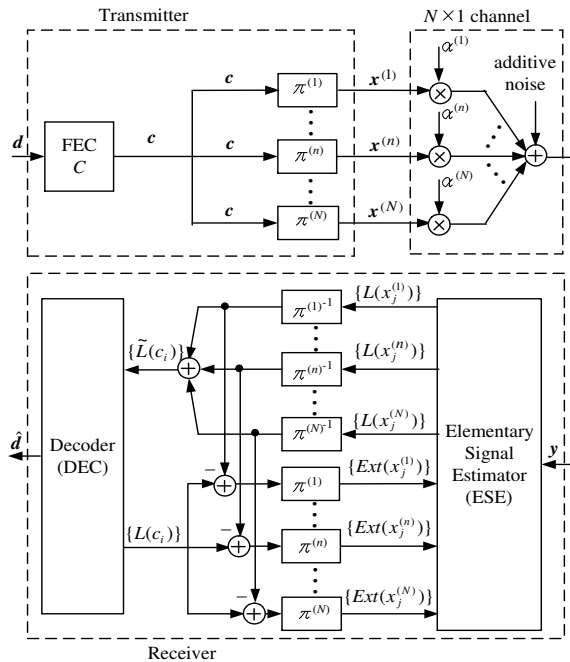


Fig. 1 Transmitter and (iterative) receiver structures of an $N \times 1$ interleaver-based space-time coding scheme with BPSK signaling. $\pi^{(n)}$ is the random interleaver for the n th transmit antenna.

be the transmitted codeword matrix, with $\mathbf{x}^{(n)}$ assigned to the n th transmit antenna. The signal received at time j is given by

$$y_j = \sum_{n=1}^N \alpha^{(n)} x_j^{(n)} + n_j, \quad (2)$$

where n_j is a zero mean complex Gaussian random variable with variance $\sigma^2 = N_0/2$ per dimension.

First we consider binary-phase-shift-keying (BPSK) signaling. Fig. 1 shows the transmitter and (iterative) receiver structures of an $N \times 1$ interleaver-based space-time coding scheme with BPSK signaling. The information sequence \mathbf{d} is first encoded by a binary FEC code C , generating a sequence \mathbf{c} over $\{+1, -1\}$. The coded sequence \mathbf{c} is then independently interleaved N times using N random interleavers $\{\pi^{(1)}, \dots, \pi^{(n)}, \dots, \pi^{(N)}\}$, producing $\{\mathbf{x}^{(1)}, \dots, \mathbf{x}^{(n)}, \dots, \mathbf{x}^{(N)}\}$ to be transmitted simultaneously from N antennas. The basic principle of this scheme is that $\pi^{(n)}$ should be different for different n so as to reduce the correlation among signals on different antennas.

Quadrature-phase-shift-keying (QPSK) signaling can also be used. In this case, each interleaved version of \mathbf{c} is divided into two equal-length sub-sequences to form the real and imaginary parts of $\mathbf{x}^{(n)}$ ($n=1, \dots, N$). In this way, the overall transmission rate doubles.

3. Receiver Structure

The random interleavers used in Fig. 1 ensure that the interference among signals from different antennas is diversified in time. Due to the repetition operation used, the information carried by each bit in \mathbf{c} is now gathered from N time samples. This reduces the likelihood of worst-case scenarios such as signals from different antennas canceling each other out completely for a certain bit. The strategy is somewhat similar to that used in code-division multiple-access (CDMA) systems for alleviating cross-cell interference. We now devise a very efficient turbo-type [21] detection mechanism based on multiuser detection principles for CDMA [22].

For simplicity and clarity, we first discuss in 3.1 ~ 3.3 the situation for BPSK signaling and real α . Later in 3.4, we will generalize the results to QPSK signaling and complex α .

3.1 Overview of the Receiver

The system model in Fig. 1 is restricted by two constraints, namely the FEC code C and the channel constraint α . The receiver function is to estimate the original information \mathbf{d} based on the channel observations $\mathbf{y} = \{y_j\}$ and the two constraints. Finding an optimal solution is usually prohibitively complicated, so we will resort to a sub-optimal method. A basic strategy is to consider the two constraints separately, as depicted in Fig. 1 and outlined below, and then combine the results in an iterative manner [21].

The iterative receiver shown in Fig. 1 consists of an Elementary Signal Estimator (ESE) and an *a posteriori* probability (APP) decoder (DEC). The two constraints mentioned above are used separately in the ESE and DEC, and their results are combined using a turbo-type iterative process [21]. This greatly reduces the complexity.

In the ESE, only the channel constraint α is considered. The ESE generates coarse estimates $\mathbf{L} \equiv \{L(x_j^{(n)}), \forall n, j\}$ for $\{x_j^{(n)}, \forall n, j\}$, where

$$L(x_j^{(n)}) \equiv \log \left(\frac{p(y_j | x_j^{(n)} = +1, \alpha)}{p(y_j | x_j^{(n)} = -1, \alpha)} \right), \quad \forall n, j. \quad (3)$$

Note that each bit c_i in \mathbf{c} has N replicas in $\{x_j^{(n)}, \forall n, j\}$. Let $S(c_i)$ be the index set of these N replicas (for all (n, j) combinations). The information from all bits in $S(c_i)$ is collected to produce the estimate $\tilde{L}(c_i)$ for c_i , where

$$\tilde{L}(c_i) \equiv \sum_{(n,j) \in S(c_i)} L(x_j^{(n)}), \quad \forall i. \quad (4)$$

The DEC then uses $\{\tilde{L}(c_i), \forall i\}$ as the *a priori*

information of \mathbf{c} to calculate the *a posteriori* log-likelihood ratios (LLRs) $\{L(c_i), \forall i\}$ of \mathbf{c} based on the constraint of C , where

$$L(c_i) \equiv \log \left(\frac{\Pr(c_i = +1 | \mathbf{L}, C)}{\Pr(c_i = -1 | \mathbf{L}, C)} \right), \quad \forall i. \quad (5)$$

The feedback from the DEC to the ESE is the extrinsic information $\{Ext(x_j^{(n)}), \forall n, j\}$ for $\{x_j^{(n)}, \forall n, j\}$, defined as

$$Ext(x_j^{(n)}) \equiv \log \left(\frac{\Pr(x_j^{(n)} = +1 | \mathbf{L}, C)}{\Pr(x_j^{(n)} = -1 | \mathbf{L}, C)} \right) - L(x_j^{(n)}), \quad \forall n, j. \quad (6)$$

Here the use of extrinsic information follows the turbo principle [21], i.e., the information generated by the ESE should be avoided from circulating back to the ESE again. This extrinsic information can be calculated by extracting $L(x_j^{(n)})$ from $L(c_i)$ (assuming $(n, j) \in S(c_i)$)

$$Ext(x_j^{(n)}) = L(c_i) - L(x_j^{(n)}), \quad \forall n, j. \quad (7)$$

The ESE and DEC functions are carried out iteratively. After the final iteration, the DEC produces hard decisions $\hat{\mathbf{d}}$ on the information sequence \mathbf{d} based on $\{L(c_i)\}$.

The DEC performs a standard APP decoding of C [21], and we only consider the ESE function below.

3.2 The ESE Function

The basic function of the ESE is to resolve CAI. The constraint C is not considered here in order to reduce complexity.

We use $Ext(x_j^{(n)})$ (initialized to zero) to approximate the *a priori* LLR of $x_j^{(n)}$, i.e.,

$$\log \left(\frac{\Pr(x_j^{(n)} = +1)}{\Pr(x_j^{(n)} = -1)} \right) \approx Ext(x_j^{(n)}), \quad \forall n, j. \quad (8)$$

Based on (2), the optimal solution to (3) is

$$L(x_j^{(n)}) = \log \left(\frac{\left(\sum_{\substack{m=1 \\ m \neq n}}^N p(y_j | x_j^{(1)} = \pm 1, \dots, x_j^{(n)} = +1, \dots, x_j^{(N)} = \pm 1, \boldsymbol{\alpha}) \prod_{\substack{m=1 \\ m \neq n}}^N \Pr(x_j^{(m)} = \pm 1) \right)}{\left(\sum_{\substack{m=1 \\ m \neq n}}^N p(y_j | x_j^{(1)} = \pm 1, \dots, x_j^{(n)} = -1, \dots, x_j^{(N)} = \pm 1, \boldsymbol{\alpha}) \prod_{\substack{m=1 \\ m \neq n}}^N \Pr(x_j^{(m)} = \pm 1) \right)} \right) \quad \forall n, j. \quad (9)$$

The summations in the numerator and denominator in (9) are over all possible $(x_j^{(1)}, \dots, x_j^{(N)})$ with $x_j^{(n)}$ fixed to be +1 and -1 respectively. $\Pr(x_j^{(n)} = \pm 1)$ is the *a priori* probability of $x_j^{(n)}$ being ± 1 , which can be calculated from (8) as

$$\Pr(x_j^{(n)} = +1) = \frac{\exp(Ext(x_j^{(n)}))}{1 + \exp(Ext(x_j^{(n)}))}, \quad \forall n, j, \quad (10a)$$

$$\Pr(x_j^{(n)} = -1) = \frac{1}{1 + \exp(Ext(x_j^{(n)}))}, \quad \forall n, j. \quad (10b)$$

The complexity of (9) grows exponentially with the number of transmit antennas N . For large N , the calculation of (9) is very difficult. To reduce complexity, we consider a sub-optimal solution to (3) as follows. We treat $x_j^{(n)}$ as a random variable. Denote by $E(\bullet)$ and $\text{Var}(\bullet)$ the mean and variance functions, respectively. The mean and variance of $x_j^{(n)}$ can be calculated from (8) as

$$E(x_j^{(n)}) \approx \frac{\exp(Ext(x_j^{(n)})) - 1}{\exp(Ext(x_j^{(n)})) + 1} = \tanh(Ext(x_j^{(n)})/2), \quad \forall n, j, \quad (11a)$$

$$\text{Var}(x_j^{(n)}) = 1 - (E(x_j^{(n)}))^2, \quad \forall n, j. \quad (11b)$$

Denoting $\zeta_j^{(n)} = \sum_{\substack{m=1 \\ m \neq n}}^N \alpha^{(m)} x_j^{(m)} + n_j$, the j th

received signal can be written as

$$y_j = \alpha^{(n)} x_j^{(n)} + \zeta_j^{(n)}. \quad (12)$$

The Gaussian Approximation: Applying the Central Limit Theorem, $\zeta_j^{(n)}$ in (12) can be approximated by a Gaussian random variable with mean and variance

$$E(\zeta_j^{(n)}) = E(y_j) - \alpha^{(n)} E(x_j^{(n)}), \quad (13a)$$

$$\text{Var}(\zeta_j^{(n)}) = \text{Var}(y_j) - \left| \alpha^{(n)} \right|^2 \text{Var}(x_j^{(n)}), \quad (13b)$$

where (based on (2))

$$E(y_j) = \sum_{m=1}^N \alpha^{(m)} E(x_j^{(m)}), \quad (14a)$$

$$\text{Var}(y_j) = \sigma^2 + \sum_{m=1}^N \left| \alpha^{(m)} \right|^2 \text{Var}(x_j^{(m)}). \quad (14b)$$

The Central Limit Theorem applies to the sum of a reasonably large number of independent random variables. When N is small, the Gaussian Approximation

may be inaccurate. Nevertheless, we observe from simulation results that the Gaussian Approximation works well even for $N = 2$, as will be illustrated in Fig. 2. Note that the simulation results are all based on QPSK signaling. (The detection algorithm with QPSK signaling will be discussed in 3.4.) In this case, the number of interfering signals (including both real and imaginary parts) is $2N-1$, rather than $N-1$ as for BPSK signaling.

Applying the Gaussian Approximation to (12), (3) can be calculated as,

$$\begin{aligned} L(x_j^{(n)}) &= \log \left(\frac{\exp \left(-\frac{(y_j - \mathbb{E}(\zeta_j^{(n)}) - \alpha^{(n)})^2}{2\text{Var}(\zeta_j^{(n)})} \right)}{\sqrt{2\pi\text{Var}(\zeta_j^{(n)})}} \right) \\ &\quad - \log \left(\frac{\exp \left(-\frac{(y_j - \mathbb{E}(\zeta_j^{(n)}) + \alpha^{(n)})^2}{2\text{Var}(\zeta_j^{(n)})} \right)}{\sqrt{2\pi\text{Var}(\zeta_j^{(n)})}} \right) \\ &= 2\alpha^{(n)} \cdot \frac{y_j - \mathbb{E}(\zeta_j^{(n)})}{\text{Var}(\zeta_j^{(n)})}, \quad \forall n, j. \end{aligned} \quad (15a)$$

Substituting (13) to (15a), we have

$$L(x_j^{(n)}) = 2\alpha^{(n)} \cdot \frac{y_j - \mathbb{E}(y_j) + \alpha^{(n)}\mathbb{E}(x_j^{(n)})}{\text{Var}(y_j) - |\alpha^{(n)}|^2 \text{Var}(x_j^{(n)})}, \quad \forall n, j. \quad (15b)$$

It can be shown that the complexity involved in (15b) grows only linearly with N . Compared with the optimal solution, the sub-optimal one has much lower complexity with large N , and is more flexible for systems with large numbers of transmit antennas. In Section 4, we will use simulation results to show that the sub-optimal solution can achieve similar performance to the optimal one.

In the remainder of this paper, we will always assume that the Gaussian Approximation is used in the ESE, unless stated otherwise.

3.3 A Summary of the Detection Algorithm

For clarity, we summarize the (real) detection algorithm discussed above as follows.

(a) Initialization: Set $Ext(x_j^{(n)}) = 0$. $\forall n, j$.

(b) Main iteration:

$$\mathbb{E}(x_j^{(n)}) = \tanh(Ext(x_j^{(n)})/2), \quad \forall n, j. \quad (16a)$$

$$\text{Var}(x_j^{(n)}) = 1 - (\mathbb{E}(x_j^{(n)}))^2, \quad \forall n, j. \quad (16b)$$

$$\mathbb{E}(y_j) = \sum_{n=1}^N \alpha^{(n)} \mathbb{E}(x_j^{(n)}), \quad \forall j. \quad (17a)$$

$$\text{Var}(y_j) = \sigma^2 + \sum_{n=1}^N |\alpha^{(n)}|^2 \text{Var}(x_j^{(n)}), \quad \forall j. \quad (17b)$$

$$L(x_j^{(n)}) = 2\alpha^{(n)} \cdot \frac{y_j - \mathbb{E}(y_j) + \alpha^{(n)}\mathbb{E}(x_j^{(n)})}{\text{Var}(y_j) - |\alpha^{(n)}|^2 \text{Var}(x_j^{(n)})}, \quad \forall n, j. \quad (18)$$

$$\tilde{L}(c_i) = \sum_{(n,j) \in S(c_i)} L(x_j^{(n)}), \quad \forall i. \quad (19)$$

The APP decoding of C in the DEC is performed at this point using $\{\tilde{L}(c_i)\}$ as the input so that $\{L(c_i)\}$ are available,

$$Ext(x_j^{(n)}) = L(c_i) - L(x_j^{(n)}), \quad \forall n, j. \quad (20)$$

Then go back to (16) for the next iteration.

The computational cost of the operations involved in (16) ~ (20) is, excluding the decoding of C , about $8N$ additions, $6N$ multiplications and N $\tanh(x)$ functions per coded bit per iteration. If C is a turbo-type code, the DEC may contain internal iterations. These internal iterations can be incorporated into the global iteration described above, e.g., one internal iteration per global iteration. Since the other costs are so low, the overall receiver complexity is dominated by the APP decoding of C .

3.4 Generalization

The derivations in 3.1 ~ 3.3 are for BPSK signaling and real α . We now show that the basic detection principle remains the same when these restrictions are removed.

- (i) Consider complex α and BPSK signaling. Except for a 90° phase shift, we can simply treat the imaginary part of the arrival signal in the same way as the real part from an extra receive antenna. In this case, (16) ~ (18) should be carried out twice based on the real and imaginary parts respectively. Eqn. (19) should be modified to gather information for each c_i from both real and imaginary parts of its N observations. Eqn. (20) should also be modified accordingly.
- (ii) With complex α and QPSK signaling, the imaginary parts of the transmitted signals can be seen as equivalent to the real parts from N extra transmit antennas with a 90° phase shift.
- (iii) Combining (i) and (ii), an $N \times 1$ system with complex α and QPSK signaling can be treated similarly to a $2N \times 2$ system with real α and BPSK signaling.

From the above discussion, it can be shown that the complexity of a generalized iterative receiver is, excluding the decoding of C , about $16N$ additions, $12N$ multiplications and $2N$ $\tanh(x)$ functions per coded bit per iteration.

It can be proved that with BPSK signaling, real channel coefficients and one receive antenna, the detection algorithm discussed above is a special case of

the minimum mean-square error and soft interference cancellation (MMSE-IC) algorithm [10][23][24] (without spreading sequences). For QPSK signaling, complex channel coefficients and one receive antenna, the above detection algorithm differs from the MMSE-IC algorithm in that a real representation is used to deal with complex signals. In this way, the two bits in the real and imaginary parts of a complex signal can have their individual variances, which leads to a performance improvement. (For detailed discussions, please refer to [25].)

4. Numerical Results

In this section, we present some simulation results to demonstrate the performance of the proposed scheme. We refer to the new codes as Interleave-Division-Multiplexing (IDM) codes [26] due to their connection to the Interleave-Division Multiple-Access (IDMA) scheme [22]. QPSK signaling and complex α are always assumed. The interleavers used in simulation are all generated independently and randomly. We adopt the following notations,

- N_{info} = number of information bits in a frame,
- R = number of information bits per channel use,
- It = iteration number, and
- E_b = average energy per information bit.

Assume no channel state information (CSI) at the transmitter and ideal CSI at the receiver. Denote by ρ the average received signal-to-noise ratio (SNR). The capacity of an $N \times 1$ system for any given α is [4] $C(\alpha) = \log(1 + \frac{\rho}{N} \alpha \alpha^H)$, where α^H is the Hermitian of α . $C(\alpha)$ is a random variable depending on α . If $C(\alpha)$ falls below the overall transmission rate R , reliable communication is impossible. Such an event is referred to as an outage. The outage capacity is defined as [27] $P_{\text{out}} \equiv \Pr(C(\alpha) < R)$ that can be calculated based on the distribution of α . The outage capacity serves as a theoretical limit of the frame-error-rate (FER) performance of an $N \times 1$ system, and we will use it as a benchmark in our simulation.

Fig. 2 illustrates the FER performance of $N \times 1$ IDM codes with (a) $R = 2/3$ bits per channel use and (b) $R = 1$ bit per channel use in quasi-static Rayleigh fading channels using both the optimal solution in (9) (only for $N = 2$ and 4)^{††} and the sub-optimal one in (15) for bit estimation in the ESE. With $R = 2/3$, a rate-1/3 (15, 13)₈ turbo code is used as the FEC code C , and with $R = 1$, a punctured rate-1/2 (15, 13)₈ turbo code is used. Corresponding outage capacities are included for reference. From this figure, we can see that the sub-optimal approach using the Gaussian Approximation can achieve almost the same performance as the optimal one, while the related complexity is greatly reduced (especially for large N). Therefore, the sub-

^{††}For $N = 8$, the complexity involved is too high.

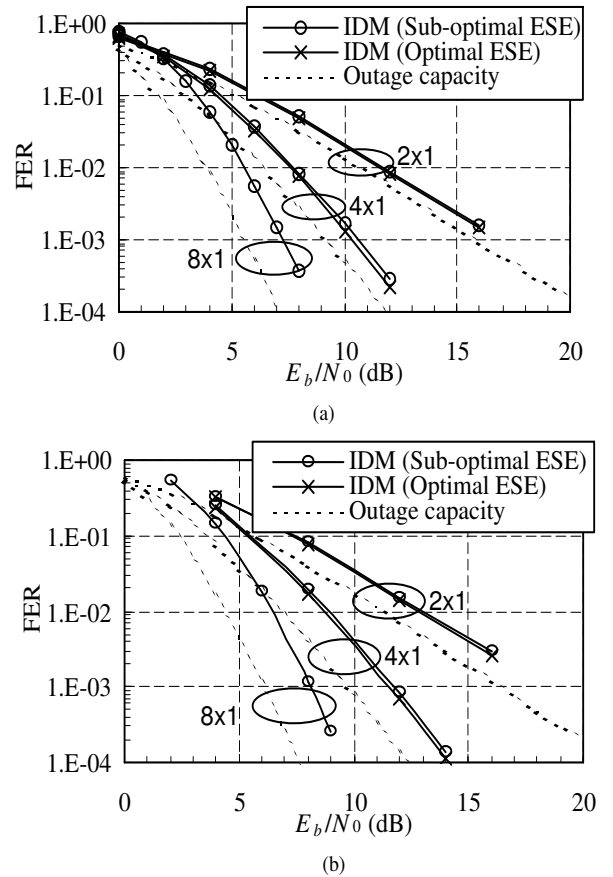


Fig. 2 FER performance of $N \times 1$ IDM codes with (a) $R = 2/3$ and (b) $R = 1$ in quasi-static Rayleigh fading channels using both the optimal and sub-optimal solutions for bit estimation in the ESE. $N_{\text{info}} = 512$. $It = 10$. A rate-1/3 and a rate-1/2 (15, 13)₈ turbo codes are used as the FEC code. The corresponding outage capacities are included for reference. The antenna numbers are marked on the figures.

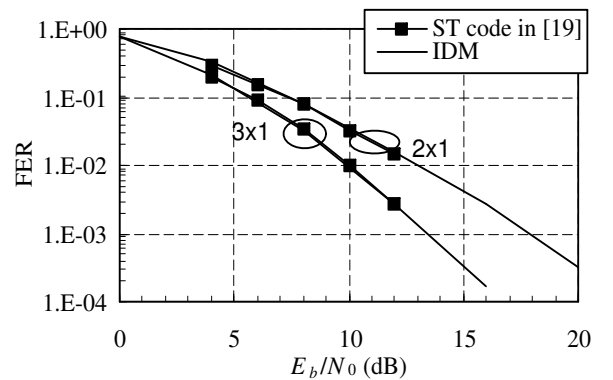


Fig. 3 FER performance comparison between the IDM codes and the space-time codes in [19] with $N = 2$ and 3. All the codes have $R = 1$ bit per channel use. The IDM codes have $N_{\text{info}} = 512$, $It = 10$, and use a rate-1/2 (15, 13)₈ turbo code as the FEC code.

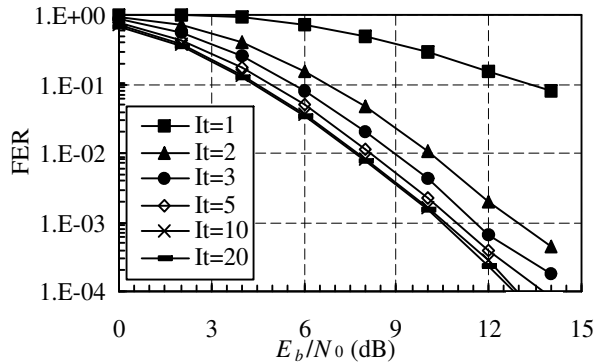


Fig. 4 Convergence property of the IDM code in Fig. 2(a) with $N = 4$.

optimal approach will be used for all the simulation results below. We can also see that the FER curves of the IDM codes are only about 0.7~2dB away from the corresponding outage capacities.

Fig. 3 compares the FER performance between IDM codes and one of the best space-time codes known to the authors [19]. All the codes have $R = 1$ bit per channel use. It is observed that the IDM code and the code in [19] have similar performance with $N = 2$ and 3. However, the design of the code in [19] becomes complicated with large N . In this case, the IDM code provides a conceptually simpler alternative, which is more flexible for systems with arbitrary numbers of transmit antennas. Another interesting observation is that the FER performance curves of the IDM code and the code in [19] have the same asymptotic slopes. Note that the asymptotic slopes show the diversity degrees achieved by the corresponding codes, and the code in [19] has full diversity. It seems that with random interleaving and repetition coding, the IDM code can nearly achieve full diversity without sophisticated design strategy.

Fig. 4 shows the convergence property of the IDM code in Fig. 2(a) with $N = 4$. From this figure, we can see that the most gain can be achieved with 5 iterations.

5. Conclusions

We have presented an efficient detection technique for random-interleaver-based space-time codes. With the proposed technique, the detection complexity is very moderate, and grows only linearly with the number of transmit antennas. Thus, systems with a large number of transmit antennas can be processed.

The basic principle of the scheme in Fig. 1 is the use of repetition coding together with random interleaving and iterative detection. The repetition coding is a simple way to achieve diversity, since each bit has N replicas transmitted from N antennas with different fading coefficients. At the receiver side, the information about a bit is collected from N samples. Such a tech-

nique has been studied before, e.g., the delay diversity scheme [28]. The work in this paper shows that such a simple scheme can achieve performance close to the theoretical limit (as a result of the iterative detection strategy). This scheme is applicable to any number of transmit antennas and is simpler and more flexible than the schemes in [10][19]. (Refs [10] and [19] involve sophisticated structural design procedures and the solutions are different for different numbers of transmit antennas.)

It also appears that a codeword difference matrix in an interleaver-based code has a large probability of being full rank after random interleaving. The theoretical analysis of this problem remains open and is a subject of current investigations. (For a preliminary discussion see [26].) It will also be interesting to discover if careful design can lead to better performance for the interleaver-based code, and how much improvement can be achieved. We are currently working on this issue.

Acknowledgments

This work was fully supported by a grant from the Research Grant Council of the Hong Kong Special Administrative Region, China [Project No. CityU 1010/01E].

References

- [1] A. Wittneben, "Basestation modulation diversity for digital SIMULCAST," in Proc. IEEE VTC, 19-22 May 1991, pp. 848-853.
- [2] E. Telatar, "Capacity of multi-antenna Gaussian channels," AT&T-Bell Labs., Internal Tech. Memo., June 1995.
- [3] G. J. Foschini, "Layered space-time architecture for wireless communication in fading environment when using multiple antennas," Bell Labs Tech. J., vol. 1, pp. 41-59, Autumn 1996.
- [4] G. J. Foschini and M. Gans, "On the limits of wireless communication in a fading environment when using multiple antennas," Wireless Personal Commun., vol. 6, pp. 311-335, Mar. 1998.
- [5] V. Tarokh, N. Seshadri, and A. R. Calderbank, "Space-time codes for high data rate wireless communication: performance analysis and code construction," IEEE Trans. Inform. Theory, vol. 44, pp. 744-765, Mar. 1998.
- [6] J.-C. Guey, M. P. Fitz, M. R. Bell, and W.-Y. Kuo, "Signal design for transmitter diversity wireless communication systems over Rayleigh fading channels," IEEE Trans. Commun., vol. 47, pp. 527-537, Apr. 1999.
- [7] A. Stefanov and T. M. Duman, "Turbo coded modulation for wireless communications with antenna diversity," in Proc. IEEE VTC, Fall, vol. 3, 19-22 Sept. 1999, pp. 1565-1569.
- [8] A. Narula, M. D. Trott, and G.W. Wornell, "Performance limits of coded diversity methods for transmitter antenna arrays," IEEE Trans. Inform. Theory, vol. 45, pp. 2418-2433, Nov. 1999.
- [9] Shiu Da-Shan, G. J. Foschini, M. J. Gans, and J. M. Kahn, "Fading correlation and its effect on the capacity of multi-element antenna systems," IEEE Trans. Commun., vol. 48, pp. 502-513, Mar. 2000.